ELSEVIER

Journal of Molecular Catalysis A: Chemical 186 (2002) 89–100

JOURNAL OF MOLECULAR CATALYSIS A: CHEMICAL

www.elsevier.com/locate/molcata

Decamolybdodicobaltate(III) heteropolyanion: structural, spectroscopical, thermal and hydrotreating catalytic properties

Carmen I. Cabello*, Franco M. Cabrerizo, Alberto Alvarez, Horacio J. Thomas

Centro de Investigación y Desarrollo en Procesos Catalíticos, CINDECA, CONICET—Facultad de Ciencias Exactas, Universidad Nacional de la Plata, calle 47 No. 257, (1900), La Plata, Argentina

Received 24 September 2001; accepted 4 January 2002

Abstract

The ammonium decamolybdodicobaltate(III) salt: $(NH_4)_6[Co_2Mo_{10}O_{38}H_4]\cdot 7H_2O$ (here in Co_2Mo_{10}) has been prepared and characterized. Then, their structural, spectroscopic and thermal properties have been investigated by some physical–chemical techniques as XRD, FT-IR, Raman, DRS, SEM–EDAX,TG, DTA, and temperature programmed reduction (TPR). According to these properties, some Co_2Mo_{10}/γ-Al_2O_3 catalysts have been prepared by equilibrium impregnation of the support with aqueous solution of ammonium salts. The Co_2Mo_{10} isothermal adsorption on γ-Al_2O_3 at room temperature has been also investigated in the Mo range of 15–150 μmol Mo/ml. The hydrotreating (HDS of thiophene and HYD of cyclohexene) catalytic activity has been compared to both γ-Al_2O_3 supported Anderson phase $[(NH_4)_3[CoMo_6O_{24}H_6]\cdot 7H_2O$ (here in $CoMo_6$)] and Co–Mo conventional catalysts. The improving of activity for the Co_2Mo_{10} and $CoMo_6$ based catalysts is related to the heteropolyoxometalates adsorption process as to preparative conditions; whereas, the different activity between heteropoly-systems are undoubtedly related to the particular structure of the Co_2Mo_{10} heteropolyanion.

Keywords: Co–Mo/γ-Al_2O_3 hydrotreating catalysts; Heteropolyoxometalates; Ammonium; Decamolybdodicobaltate(III)

1. Introduction

The development, characterization and exploitation of new catalysts based on heteropolyoxocompounds are exceptionally active and of fast expansion fields. The recently observed interest in such compounds is mainly centered on Keggin or Dawson species and on their acids of great use in heterogeneous and homogeneous catalysts [1]. However, there is a long Anderson type heteropolymolybdate and tungstate specie with important structural redox and thermal properties [2–5]. These structures have shown to be bi- or tri-metallic oxide-precursor and either supported or as bulks they can be employed in some catalitic processes [6–11].

In a general project for HPAc and HPOMs study and their use in heterogeneous catalyst, the ammonium decamolybdodicobaltate(III) salt (here in Co_2Mo_{10}) has been prepared. Its heteropolyanion structure is related to Anderson type hexamolybdocobaltate(III) anion whose planar anion of D_3d symmetry was previously described in literature [2].

The scarce information about Co_2Mo_{10} anion is limited to Evans and Showel study [12]. These authors described this structure as derived from Co(III) Anderson phase and formed by joining two planar $CoMo_5$ specie resulting from the remotion of two MoO_2 groups from two $CoMo_6$ Anderson planar rings. In this arrangement, two octahedral CoO_6 groups occupy the

* Corresponding author. Fax: +54-221-4254277.
E-mail address: ccabello@quimica.unlp.edu.ar (C.I. Cabello).

1381-1169/02/$ – see front matter
PII: S1381-1169(02)00043-2

center of the heteropolyanion. All these structural features seem to have promising catalytic properties since the Co:Mo ratio is higher for Co_2Mo_{10} than for $CoMo_6$ which has been successfully used for the preparation of hydrotreating Co–Mo/γ-Al_2O_3 type catalysts [6].

This last system has some advantages over the conventional hydrotreating catalysts such as the supression of calcination steps during the activation proccess. It is well-known that $CoAl_2O_4$ specie is formed during the thermal process therefore the decrease of active Co occurs [13]. On the other hand, the planar ring adsorption is good, leading to a catalyst with 8% of Mo and 0.8% of Co adsorbed (g Mo/100 g/Al_2O_3) and Co/[Co + Mo] = 0.14 ratio [6]. This catalyst has an activity which can be compared to the conventional catalyst activity. The purpose of this paper is to study the Co_2Mo_{10} heteropolyanion from its structural spectroscopic properties and its adsorption in alumina to be used as a precursor on hydrotreating process. Since there are no previous works about Co_2Mo_{10} in the catalysis field, the comparative study on Anderson phase results has been made. An attempt to establish some type of correlations between hydrotreating activity of supported Co_2Mo_{10} and structural, spectroscopical and thermal properties, XRD, SEM–EDAX, DRS, FT-IR, Raman and DTA–TGA physical–chemical techniques were employed on bulk and/or supported samples. Taking all these properties into account, the isothermal adsorption and the hydrotreating activity (HDS, HYD here in H_S and H_Y, respectively) of γ-Al_2O_3-supported Co_2Mo_{10} have been studied.

The hydrodesulfurization activity for the system under study is higher than the same activity for the $CoMo_6$ based system. In addition, the hydrogenation activity for Co_2Mo_{10} is higher than the same activity for commercial catalyst.

In this work, all these results are discussed on the basis of some important aspects: (a) heteropolyanion structural characteristics which give a higher reactivity to the catalyst surface; (b) catalysts preparation and activation.

2. Experimental

2.1. Synthesis and characterization of pure phase

The synthesis of the ammonium salt of decamolybdocobaltate(III) (Co_2Mo_{10}) was carried out by the slow precipitation from ammonium heptamolybdate (hereafter AHM) solutions and $Co(NO_3)_2$ in stoichiometric amounts and oxidant appropriate conditions, according to the general method previously described [12]. The characterization of the species was carried out by X-ray powder diffraction (XRD), by means of a Philips PW 1714 diffractometer (Cu Kα radiation, Ni filter), and by infrared and Raman spectroscopy by means of a Bruker IFS 66 FT-IR spectrophotometer (KBr pellet technique) and a Bruker FTIFS interpherometer (Nd-YAG laser, 1064 μ), respectively. Samples were also observed by scanning electron microscopy SEM using a Philips 505 electron microscope with an EDAX 9100 microsonde and energy dispersive detector.

2.2. Thermal analysis

TG and DTA measurements were carried out on a Shimadzu Thermoanalyzer (TGA-50 and DTA-50) working in an N_2 stream. The heating rate was 10 °C min^{-1} and the temperature was raised up to 1000 °C.

Additional thermal studies were carried out in a furnace, using similar conditions to those of the DTA–TG measurements. These experiments provide a characterization of intermediate and pyrolysis residues.

2.3. Analysis by TPR

The TPR patterns of the ammonium salt of Co_2Mo_{10} were obtained by means of a home-made equipment. The reactor was fed with 10% of H_2 reducing agent in N_2 (100 cm^3 min^{-1}) from 20 to 1000 °C. The heating rate was 10 °C min^{-1}. Similar TPR conditions were used in order to compare the present results with those previously obtained for pure $CoMo_6$ Anderson phases [5]. The consumed H_2 was detected by a conductimetric cell.

2.4. Adsorption isotherm and catalysts preparation

The adsorption isotherm of Co_2Mo_{10} ammonium salt on γ-Al_2O_3 supports was obtained by the equilibrium impregnation of the support from salt aqueous solutions with concentrations from 15–150 μmol Mo/ml.

The γ-Al_2O_3 powder support presents superficial area of 226 m^2/g, pore volume of 0.65 cm^3/g and a grain size of 200 μm. The impregnation was performed at room temperature with excess of solution, in a continuous stirring for 24 h. Then, the solid was separated by centrifugation and it was dried in the heater at 80 °C. The chemical analysis of the solutions before and after the impregnation were made by IL-457 atomic absorption spectrometer. With these results, the C_i (initial impregnant solution) and C_f (final impregnant solution) concentrations, expressed in mg metal/ml of solution were calculated. From these values and by means of a simple matter balance equation, it was possible to calculate C_a (adsorbed concentration of metal, such as Mo or Co) expressed in g M/g support. In addition, it was possible to obtain the total Mo and Co content as C_t (g M/100 g γ-Al_2O_3) from the addition of adsorbed M(C_a) + occluded M(C_o) in the pores where C_o is the M amount could result in an increase of the active species in the drying stage. C_o was evaluated according to a theoretical model as $C_o = C_f \times V_o$, where V_o is the pore volume.

The adsorbed Mo concentration C_a, [expressed as monolayer (%)] is plotted versus the Mo concentration in the solution in equilibrium (C_f). It was found that the shape of the curve follows the Langmuir model [14,15]. Thus, by plotting the linearized form of the Langmuir equation $[C_f/C_a = (1/K_{ad}S) + (C_f/S)]$ and by extrapolating the subsequent straight line, it is possible to calculate the total number of active sites (S), expressed in g Mo/g γ-Al_2O_3. The equilibrium adsorption constant (K_{ad}) expressed in ml/g Mo may also be obtained from the slope of the line.

Similar studies have been performed with AHM (AHM(VI) tetrahydrate Aldrich) with comparative purposes.

2.5. Analysis by diffuse reflectance spectroscopy (DRS)

The characterization of the pure and supported phases as well as of the pyrolisis remainders and intermediates was carried out by a UV–VIS Varian Super Scan 3 spectrophotometer, with double beam and built-in recorder. The γ-Al_2O_3 (support used in the catalyst preparation) was used as internal standard.

2.6. Catalytic activity measurements

The thiophene hydrodesulfurization and cyclohexene hydrogenation activity of the catalysts were measured in a high pressure reactor. The selected feedstock composition was cyclohexane (90%), cyclohexene (10%) and thiophene (15,000 ppm). The experimental conditions for the activity runs were: liquid flow rate 0.353 ml min^{-1}; LHSV = 56.3 l/h; total pressure: 30 kg cm^{-2} and reaction temperature: 280 °C. The analysis of the product has been made by gas chromatography by means of a Varian Start 3400 Chromatograph, with FID detector. The catalytic activity was expressed as H_S (%) of thiophene and H_Y (%) cyclohexene conversion and calculated as the ratio from their final to the initial concentration. The samples were previously presulfurized, in situ, by using a mixture of thiophene and cyclohexene heated from RT up to 300 °C for 1 h and then the temperature was lowered to 280 °C using the technique previously described [6].

3. Results and discussion

3.1. Morphological and structural features

Fig. 1 shows the structure of the decamolybdodicobaltate(III) and Anderson heteropolyanions. The $[CoMo_6O_{24}H_6]$ group is made up of a compact package of six MoO_6 octahedra which are surrounding one XO_6 in a planar hexagonal configuration, with approximative overall D_3d symmetry. According to Evans and Showell [12], the heteropoly-molecule ion

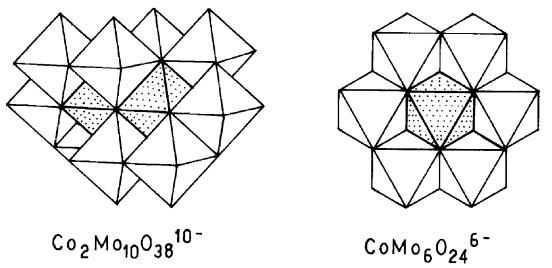

Fig. 1. Structure of the decamolybdodicobaltate (III), $[Co_2Mo_{10}O_{38}]$ and Anderson hexamolybdocobaltate (III) $[CoMo_6O_{24}]$ heteropolyanions.

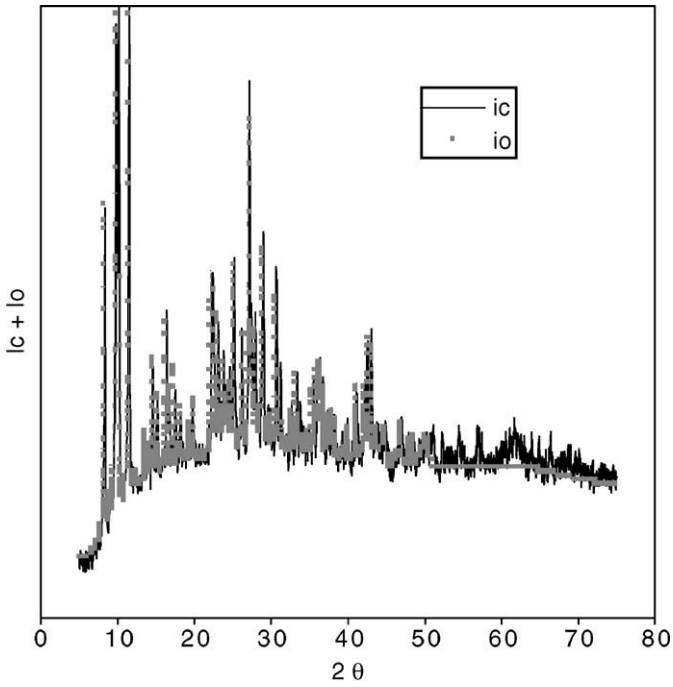

Fig. 2. Comparative XRD patterns of: (I_o) observed and (I_c) calculated for Co_2Mo_{10} ammonium salt powder.

$[H_4Co_2Mo_{10}O_{38}]$ conforms closely to an ideal point symmetry 222 (D_2) and it may be considered as being derived from the Anderson ion by removing one MoO_2 group from each of two hexa molecules, turning one 180° around CoO_6 octahedron diagonal, and joining them so that the two CoO_6 octahedra come together at the center sharing an edge. Fig. 2 shows the XRD pattern matching the observed (I_o) and calculated (I_c) spectra for Co_2Mo_{10} ammonium salt powder. The calculated data has been obtained by means of the FullProf 3.0.0 Apr 95-LLB-JRC Program [16] and the best adjustment between I_o and I_c has been obtained by using the crystalographics parameters for the form A, monoclinic, space group *C2c* or *Cc*; $a = 44.18 \pm 0.03$ Å; $b = 12.60 \pm 0.01$ Å; $c = 15.36 \pm 0.01$ Å; $\beta = 106.89 \pm 0.02°$; $Z = 8$; $V = 4 \times 2044$ Å^3 [12]. Fig. 3 shows the SEM micrographs of Co_2Mo_{10} and $CoMo_6$ crystals. A clear difference in the morphology of the samples can be appreciated. The electron microprobe analysis by EDAX for Co_2Mo_{10}, reveals a Co:Mo ratio of 1:8.5 according to the theoretical value of 1:8.14.

3.2. Spectroscopic characterization

3.2.1. Vibrational spectrum

In Table 1, it is shown the data for FT-IR and Raman vibrational spectra for Co_2Mo_{10} in 4000–400 cm^{-1} range. The assignment has been carried out taking into account the presence of different molecular unities. The spectrum can be divided into the following typical regions: (1) 3600–2800 cm^{-1} corresponding to the O–H and N–H stretchings; (2) 1700–1400 cm^{-1} the region of the O–H and N–H bendings; (3) 1000–850 cm^{-1} assignable to the Mo–O_2 terminal stretchings; (4) 750–550 cm^{-1} assignable to the Mo–O–Mo bridge stretchings (the vibrations of the Co–O_6 bonds and the water librations are also located in this last region). Between 550 and 500 cm^{-1}, it is possible to observe some bands attributable to the water librations. Below 450 cm^{-1}, the spectrum is rather difficult to analyze, the bending of the Mo–Ot and Mo–Ob bonds can be mixed with the Mo–Oc stretching vibrations. Likewise, the lattice modes are located below 300 cm^{-1}.

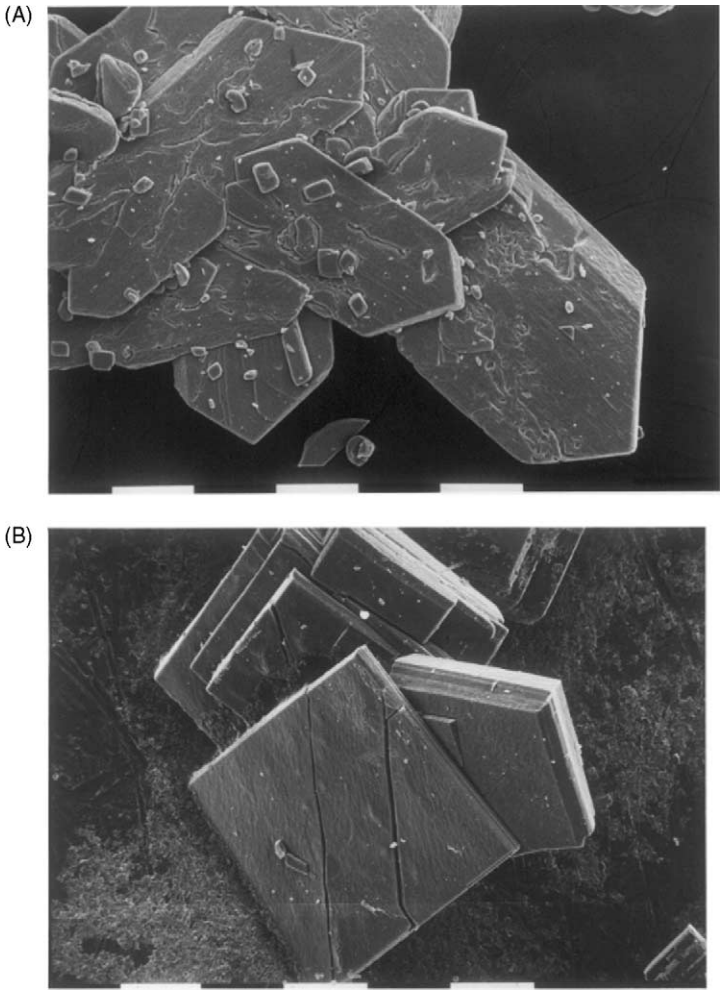

Fig. 3. SEM micrographs of ammonium salts of (A) Co_2Mo_{10} (magnification: 140×; scale bar: 100 μm) and (B) $CoMo_6$ (magnification: 200×; scale bar: 100 μm).

In Fig. 4, both FT-IR and Raman spectra, are shown. These are identical to those obtained for the $CoMo_6$ structure [3] and the FT-IR spectra are compared in Fig. 5. This study has been demonstrated that the Co_2Mo_{10} anion structure is related to the Anderson type structure which has the similar angular and bond lengths.

3.2.2. Diffuse reflectance spectra (DRS)

In Fig. 6, it is shown the DRS spectra for (a) pure specie and (b) γ-Al_2O_3 supported specie of C_t = 7.03 g Mo/100 g γ-Al_2O_3 from an aqueous solution of the Co_2Mo_{10} ammonium salt (initial concentration C_i = 150 μmol Mo/ml. The spectra show typical bands, on the UV region (200–350 nm): Mo←O charge transfer bands characteristic for octahedrical Mo(VI) centred around 270 nm. On the visible region (350–800 nm), there are two spin-allowed d–d transition bands typical for a regular octahedral configuration Co(III) (d^6) ion: ^{1}A 1g ground state to the ^{1}T 1g and ^{1}T 2g higher states, falling in the 700–550 and 500–400 nm ranges, respectively [17]. The (b) spectrum shows clearly that the heteropolyanion is adsorbed on the γ-Al_2O_3 without degradation since

Table 1
Vibrational spectrum of Co_2Mo_{10} ammonium salt

FT-IR	Raman	Assignment
3650 m	3200 w	
3484 sh		$\nu_1,\nu_3 H_2O$
3421 s		
3172 vs		$\nu_1,\nu_3 NH_4$
3024 sh		$2\nu_4$
(a) 1600 s		(a) $\delta H_2O(\nu_2)$
(b) 1404 vs		(b) $\delta NH_4(\nu_4)$
(a) 942 vs	(a) 944 vs	(a) νsMo–Ot
(b) 899 vs	(b) 901 m	(b) νaMo–Ot
858 sh		
(a) 560 sh	(a) 410 sh	(a) Lib·H_2O
(b) 442 w	(b) 398 w	(b) νMo–Oc
366 w		δM–O,
319 m	295 m	Lib·NH_4
265 sh	253 w	Lattice modes
230 sh		

Key: vs: very strong; s: strong; m: medium; w: weak; vw: very weak; sh: shoulder; br: broad.

Co(III) does not change their electronic configuration and Mo(VI) species seem to have their original octahedrical coordination for the typical polymeric species.

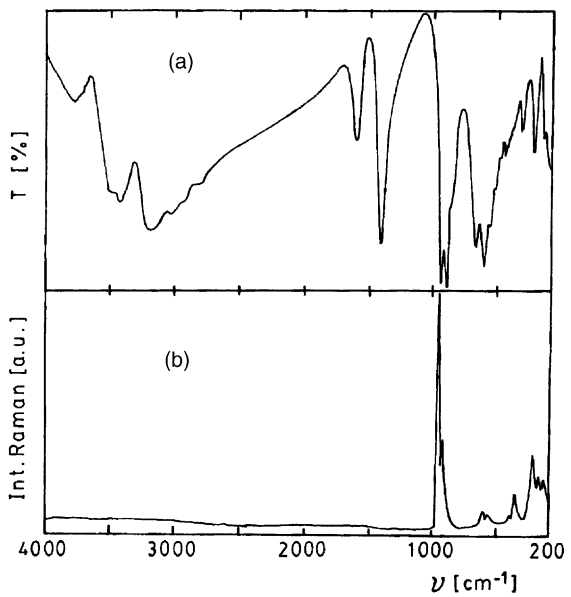

Fig. 4. (a) FT-IR and (b) Raman spectra of Co_2Mo_{10} ammonium salt (between 4000 and 200 cm^{-1}).

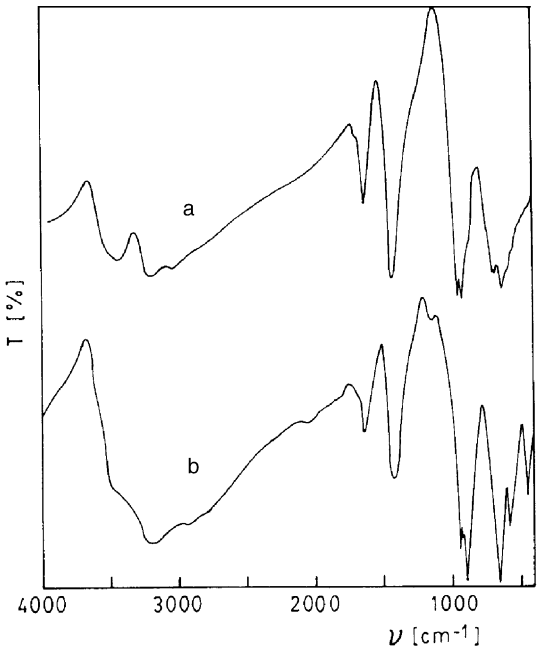

Fig. 5. Comparative FT-IR spectra of (a) Co_2Mo_{10} and (b) $CoMo_6$ ammonium salts.

3.3. Thermal behavior

3.3.1. TGA and DTA analysis

Fig. 7 shows the TG and DTA curves. It can be observed that the process occurs in five endothermic effects. The loss of crystallization water and ammonia molecules is lower compared to the analogous Anderson salt which has shown a four-step degradation thermal process [5].

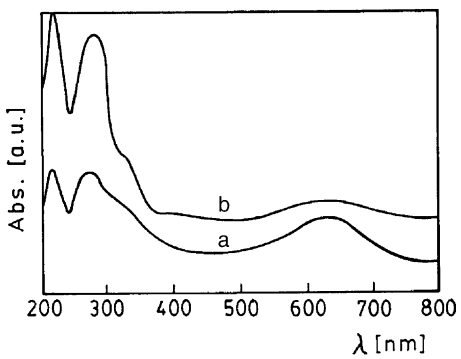

Fig. 6. Comparative DRS spectra for (a) Co_2Mo_{10} and (b) γ-Al_2O_3 supported Co_2Mo_{10} (between 200 and 800 nm).

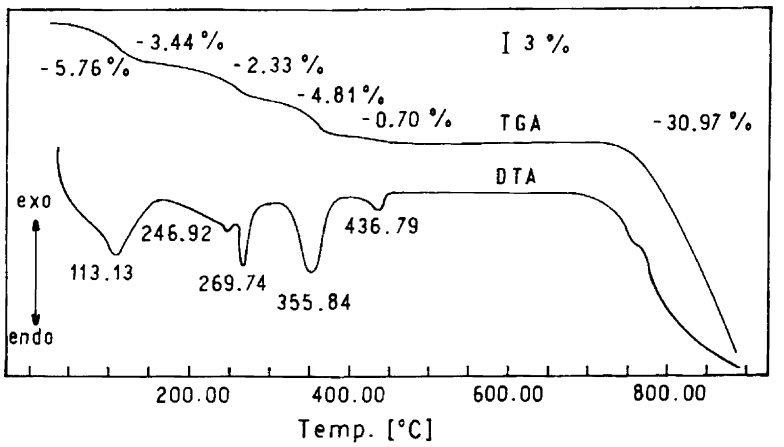

Fig. 7. TG and DTA curves for Co_2Mo_{10} ammonium salt.

In the first step, only 6.3 molecules of water are lost. The second endothermic peak at 247 °C is correlated to the loss of 3.6 molecules of water and the formation of two different species: dehydrated $[(NH_4)_3(CoMo_6H_6O_{24})]$ Anderson phase and incipient intermediated $[(NH_4)_2O]xMoO_3]{\cdot}zH_2O$ molybdic phase (PDF 23–0786). These results have been confirmed by FT-IR, XRD and SEM–EDAX complementary analysis for the sample treated in a crucible furnace at the appropriate temperature. Below 360 °C, the thermal behavior is similar to the one observed later for the Anderson phase and involves the bond rupture and the loss of both crystallization and intramolecular water. The subsequent event involves the MoO_3 and $CoMoO_4$ formation, this last specie remains as final residue of decomposition. The vibrational spectroscopy study of intermediate and pyrolysis residue show that all these are crystalline compounds. As it is observed in Fig. 8, it is revealed the presence of bands corresponding to Mo=O and Mo–O–M bonds throughout all the thermal process, starting from the Co_2Mo_{10}, following the typical MoO_3 and finishing with $CoMoO_4$ spectra.

All these conclusions lead us to formulate the following scheme:

$$(NH_4)_6[Co_2Mo_{10}H_4O_{38}] \cdot 7H_2O$$
$$\xrightarrow{113.13\,^{\circ}C} 4H_2O + \text{“}(NH_4)_4[Co_2Mo_{10}H_4O_{38}] \cdot 3H_2O\text{”}$$
$$\xrightarrow{247\,^{\circ}C} 0.5H_2O + (NH_4)_3[CoMo_6O_{24}H_6] \cdot 2.5H_2O + (NH_4) \cdot [CoMo_4O_{14}] + 2NH_3$$
$$\xrightarrow{270\,^{\circ}C} 2[(NH_4)_2O] \cdot 0.5(MoO_3 \cdot 1.75H_2O) + 2CoMoO_4 + 7MoO_3 + 3H_2O\uparrow + 2NH_3\uparrow + 0.5O_2$$
$$\xrightarrow{360\,^{\circ}C} 8MoO_3 + 2CoMoO_4 + NH_3\uparrow + 2H_2O\uparrow$$
$$\xrightarrow{437\,^{\circ}C} 8MoO_3\uparrow + 2CoMoO_4$$
$$\xrightarrow{750\,^{\circ}C} 2CoMoO_4$$

These results are in agreement with the Co_2Mo_{10} structural properties and confirm their Anderson structural relation.

3.4. TPR analysis

Because of the structural characteristics of the studied phase, the Co_2Mo_{10} TPR pattern, shown in Fig. 9, is compared with those of $CoMo_6$ and AHM. In general, the TPR behavior of the condensed molybdates exhibits two typical regions of H_2 consumption with increasing temperature. These regions correspond to Mo(VI)→ Mo(IV) and Mo(IV) → Mo(0), respectively [18]. However, it will be seen from the figure that the peak temperatures and the shapes of the patterns for the Co heteropolycompounds, differ appreciably from that of AHM. The main reason for differences is related with the presence of the Co(III) ion. In fact, the TPR patterns of HPOMs show some weak bands in the region of 300–700 °C (close to an intense band of total reduction of 800 °C), assigned to the reduction of Mo(VI) to Mo(V) and Mo(IV) and

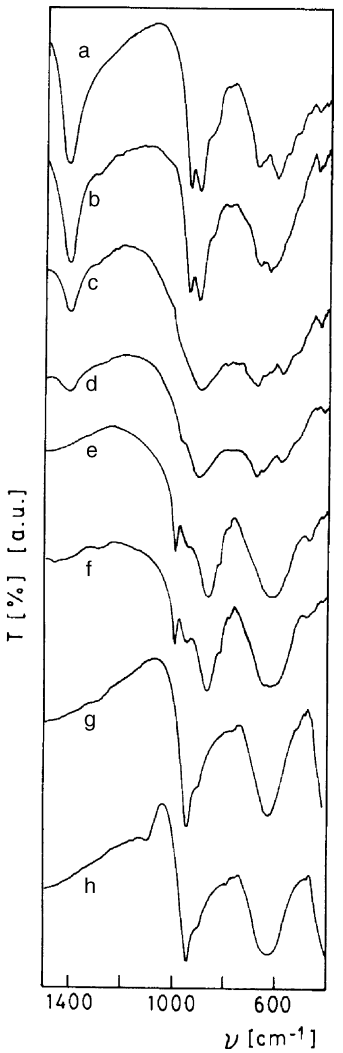

Fig. 8. Comparative FT-IR of samples of Co_2Mo_{10} corresponding to several stages of thermal treatment (in air atmosphere) from 1500 to 400 cm^{-1}. Sample heated at: (a) room temperature; (b) 120 °C; (c) 240 °C; (d) 270 °C, (e) 360 °C; (f) 440 °C; (g) 750 °C; and (h) 800 °C.

Co(III) to Co(II). Early studies about reducibility of some Anderson Phases as well as AHM, have shown that the first stage involves the formation of Mo_4O_{11} (Mo(V) containing mixed oxide) as an intermediate process which can be observed by ESR spectroscopy [5]. On the other hand, this study has clearly demonstrated that the Co ion produces a promoting effect by decreasing the reduction temperature of Mo(VI).

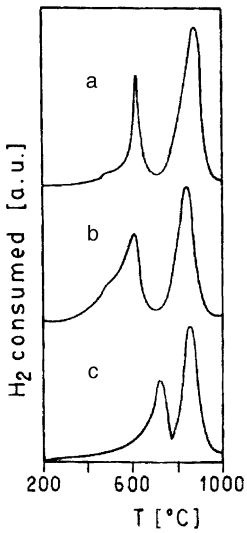

Fig. 9. TPR profiles of (a) Co_2Mo_{10}, (b) $CoMo_6$, (c) AHM.

3.5. Catalysts preparation and adsorption isotherms

The preparation of Co_2Mo_{10}/γ-Al_2O_3 catalysts were made by equilibrium impregnation of the support with aqueous solution of the ammonium salts of Co_2Mo_{10} with a Co/[Co + Mo] ratio (r) = 0.20. Fig. 10 shows the experimental results for adsorption. This isotherm shape responds to the Langmuir

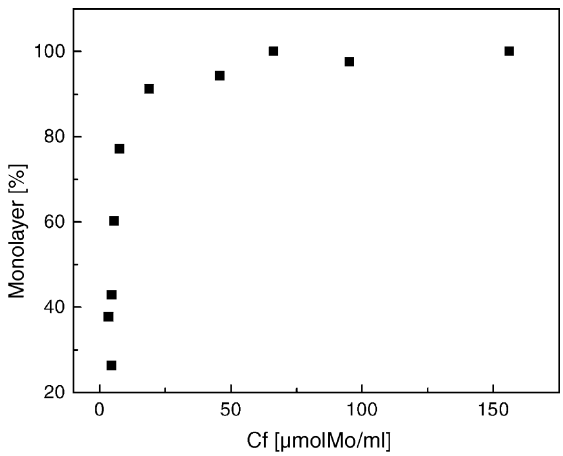

Fig. 10. Mo adsorption isotherm for Co_2Mo_{10}/γ-Al_2O_3 samples as determined at room temperature.

Table 2
Adsorption parameters for Co_2Mo_{10} and $CoMo_6/\gamma\text{-}Al_2O_3$ systems[a]

	S (g Mo_{ads} per g support)	K_{ads} (ml/g Mo)	(at. wt Mo)/(nm^2 support)	10^{23}S (at. wt Mo/g support)
Co_2Mo_{10}	0.065	1635	1.93	4.03
$CoMo_6$	0.09	1374	3.2	5.6
AHM	0.10	290	2.5	6.3

[a] $AHM/\gamma\text{-}Al_2O_3$ included for reference purposes; K_{ad} = molybdenum adsorption constant; S = number of active sites on alumina surface.

model [14,15] and such shape indicates that there is an interaction between the heteropoly anion and the support as found for the $CoMo_6$ case [6]. It can be noted that the Co content is slightly higher for the $Co_2Mo_{10}/\gamma\text{-}Al_2O_3$ than for $CoMo_6/\gamma\text{-}Al_2O_3$ where $r = 0.14$ and the adsorbed Mo content in the monolayer is lower for the first system than for the Anderson system. Then, the obtained adsorption parameters are slightly different from those of $CoMo_6$ Anderson specie. The adsorption parameters from the corresponding isotherms are given in Table 2, including the $AHM/\gamma\text{-}Al_2O_3$ data with comparative purposes. Nevertheless, the observed differences reveal that the heteropolyanions adsorption process is not so simple, involving a complex equilibrium as it has been demonstrated recently for a series of Ni(II), Co(III), Cr(III), Al(III), and Te(VI) Anderson phases [19]. These species are adsorbed as monolayer and the deposition of the D_3d Anderson anion is an ideal quasi planar deposition for Co(III) specie and a convex distortion of this symmetry for $NiMo_6$. For the Co_2Mo_{10} heteropolyanion, the symmetry (D_s) is lower than for $CoMo_6$. According to the K data for the specie under study, its deposition process seems like the corresponding Anderson anion and it is probable that the adsorption process occurs as a preferential event through any of the D_S symmetry planes of Co_2Mo_{10} heteropolyanion as it is shown in the model of Fig. 11. In addition, the lower S data indicates the lower Mo/Co stoichiometry ratio compared to the analogous $CoMo_6$ value. Likewise, the monolayer corresponds to C_t values close to 7.03 g Mo/100 g$\gamma\text{-}Al_2O_3$ (equivalent to 1.93 at. w Mo/$nm^2\gamma\text{-}Al_2O_3$). All these values are lower than those of $CoMo_6/\gamma\text{-}Al_2O_3$ [6] as it is observed in Table 2.

3.6. Catalytic activity

The operative conditions for the hydrodesulfurization of thiophene and hydrogenation of cyclohexene activity measurements, have been selected according to the recent experience about the Anderson based systems because of the common structural and thermal properties between Co_2Mo_{10} and $CoMo_6$ heteropolyanions. Therefore, the reaction temperature was 280 °C and all catalysts were presulfidate in situ at 320 °C for 1 h as it was previously established for different Anderson phases. These conditions have been established on the base of the results obtained from the thermal in both oxidizing and reducing

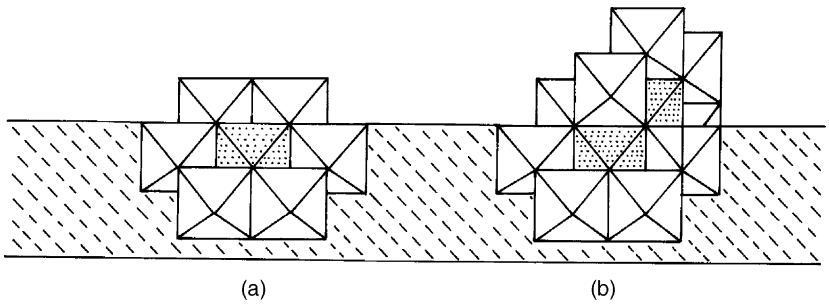

Fig. 11. Model for the ideal deposition of heteropolyanions on the support surface: (a) $CoMo_6$; (b) Co_2Mo_{10} structures.

Table 3
Chemical; H_S, H_Y conversion and Mo and Co specific activity data for different catalysts

Catalysts	C_t Co (%)	C_t Mo (%)	H_S (%)	H_S/[Mo]	H_S/[Co]	H_Y(%)	H_Y/[Mo]	H_Y/[Co]
(1) Co_2Mo_{10}/γ-Al_2O_3	1.05	7.03	75	10.67	71.43	30.90	4.40	29.43
(2) $CoMo_6/\gamma$-Al_2O_3	0.84	8.75	68	7.77	80.95	25	2.85	29.76
(3) $CoMo/\gamma$-Al_2O_3	1.80	9.30	71	7.63	39.44	28	3.01	15.55

atmospheres [5]. After the reaction temperature is reached, steady state is rapidly achieved and activity was constant in the following 8 h of reaction for both systems.

In Fig. 12a and b, it can be observed that both H_S and H_Y conversions for the Co_2Mo_{10} system have a linearly increase from $C_t = 1.70$ g Mo/100 g γ-Al_2O_3 up to $C_t = 7.03$ g Mo/100 g γ-Al_2O_3.

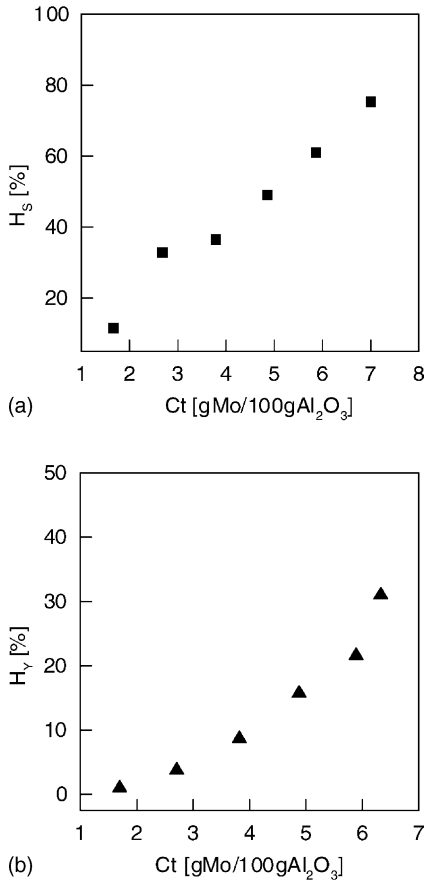

Fig. 12. Activity of the Co_2Mo_{10}/γ-Al_2O_3 catalysts in the (a) H_S; and (b) H_Y reactions.

Table 3 shows the thiophene and cyclohexene conversion and H_S/[M] and H_Y/[M] specific activity (% conversion per Co or Mo amounts) obtained by (1) γ-Al_2O_3 supported Co_2Mo_{10}; (2) γ-Al_2O_3 supported $CoMo_6$; and (3) γ-Al_2O_3 supported Co–Mo conventional catalysts and both Co and Mo concentration data for the compared samples. It is interesting to remark that the conventional catalyst has over 50% Mo loading than the Mo value for (1) and over 100% Co loading than the Co values for (2) system. However, it is observed the unexpected H_S and H_Y catalytic behavior which can be summarized by the expression (a) and (b):

$$H_S(1) > H_S(3) > H_S(2) \quad \text{(a)}$$

$$H_Y(1) > H_Y(3) > H_Y(2) \quad \text{(b)}$$

However, if the behavior of different catalysts are analyzed taking into account the specific activity, the arrangement given in (a) and (b) can be changed especially for the H_S/[Mo] and for H_Y/[Co] by the following expressions:

$$\frac{H_S}{[Mo](1)} > \frac{H_S}{[Mo](2)} \cong \frac{H_S}{[Mo](3)} \quad \text{(c)}$$

$$\frac{H_Y}{[Co](1)} \cong \frac{H_Y}{[Co](2)} > \frac{H_Y}{[Co](3)} \quad \text{(d)}$$

The (c) and (d) expressions show an undoubtedly better performance for the heteropolymetallates catalytic systems which have lower metal content. This advantage seems to be related with the adsorptive interaction process which directly depends on the HPOMs structure properties.

The impregnation process of γ-Al_2O_3 by means of heteropolymolybdate of planar or rather symmetric structure, results in a good interaction with the support leading to a uniform coverage on the surface as in $CoMo_6$ case. Also, the availability of metallic sites has been proved in our recent work about planar

D_3d symmetry $CoMo_6$ [19]. Despite the fact that in Co_2Mo_{10}, the molecule (D_2 symmetry) is not planar, it has some symmetric planes through which an adsorptive interaction could be carried out as it is shown in the model of Fig. 11. This interaction, as explained above, could be performed preferentially throughout a molecular plane being one part of the molecule without direct interaction with the support and mostly exposed to the environment.

The little symmetry of Co_2Mo_{10} causes a steric effect that may enable the formation of small molybdenita crystals, which is the active phase of the catalysts. It is well-known that this specie grows laminarly and it is even more active when the crystal is "decorated" at the edge sites by Co or Ni [20–23]. These characteristics give a greater reactivity to this catalyst surface, thus the Mo is easily sulfated, even though it has a lower Mo content compared to (2) and (3) catalysts. This result confirms the (c) expression for the hydrodesulfurization process.

As regards Co content, it can be observed that this is lower for heteropolyanion systems than for conventional catalysts with a similar Co:Mo ratio. Moreover H_Y/[Co] for (1) and (2) catalysts respectively are almost equal, which indicate that Co sites have similar accessibility for both catalysts in this process. This implies that even if there is a lower Co loading, the promoter effect is very important in the new catalysts, especially on the hydrogenation process. This fact may be due not only to above mentioned structural aspects, but also to the preparative conditions that involve the suppression of the calcination step. This enables, as it is well-known, the cobalt aluminize phase. All these aspects suggest that the obtained result for the hydrogenation process expressed in (d) is a consequence of the Co sites distribution in the new sulfide phases showing a synergic effect [24,25].

4. Conclusions

- The γ-Al_2O_3 support impregnation by HPOMs seems like an alternative method for hydrotreating catalysts preparation where HPOMs structure produces a good adsorptive interaction with the support and a uniform distribution of active sites on the catalysts surface.
- The catalytic activity for the γ-Al_2O_3 supported HPOMs is similar to that of conventional hydrotreating catalysts where $r_{\text{Commercial}} = (0.25–0.4) > r_{\text{HPOMs}} = (0.14–0.2)$ (where $r = [\text{Co}]/([\text{Co}] + [\text{Mo}])$. This fact involves the low consumption of Co but a high synergetic effect of this specie from HPOMs.
- It is observed a steric effect from the low symmetry molecules of the particular Co_2Mo_{10} catalytic systems which shows an unexpected reactive surface.
- The suppression of the calcination steps prevents the formation of $CoAl_2O_4$ spinel and then the inactive cobalt.

Acknowledgements

C.I. Cabello is a member of the research staff of CICPBA, Argentina. This work was supported by CONICET and CICPBA. The authors thank Mrs. Graciela Valle, Mr. N. Firpo and Mr. D. Peña for technical assistance.

References

[1] (a) N. Mizuno, M. Misono, Chem. Rev. 98 (1998) 199;
(b) M.T. Pope, A. Müller, Polyoxometalate Chemistry from Topology via Self-assembly to Applications, Kluwer Academic Publishers, London, 2001;
(c) P. Vazquez, L. Pizzio, C. Cáceres, M. Blanco, H. Thomas, E. Alesso, L. Finkielsztein, B. Lantaño, G. Moltrasio, J. Aguirre, J. Mol. Catal. A 161 (2000) 223;
(d) L. Briand, H. Thomas, G. Baronetti, Appl. Catal. A 201 (2000) 191.
[2] M.T. Pope, Heteropoly and Isopolyoxometalates, Springer, Berlin, New York, 1983.
[3] I.L. Botto, A.C. García, H.J. Thomas, J. Phys. Chem. Solids 53 (1992) 1075.
[4] I.L. Botto, A.C. García, H.J. Thomas, J. Latin Am. Appl. Res. 23 (1993) 113.
[5] C.I. Cabello, I.L. Botto, H.J. Thomas, Thermochim. Acta 232 (1994) 183.
[6] C.I. Cabello, I.L. Botto, H.J. Thomas, Appl. Catal. A: Gral. 197 (2000) 79.
[7] I.L. Botto, C.I. Cabello, H.J. Thomas, Mater. Chem. Phys. 47 (1997) 37.
[8] D.J. Kondaries, K. Tomishige, Y. Nagasawa, U. Lee, Y. Iwasawa, J. Mol. Catal. A 111 (1996) 145.
[9] T. Liu, K. Asakura, U. Lee, Y. Matsui, Y. Iwasawa, J. Catal. 135 (1992) 367.
[10] A.M. Maitra, N.W. Cant, D.L. Trimm, Appl. Catal. 48 (1989) 187.

[11] K. Tomishige, Y. Nagasawa, U. Lee, Y. Iwasawa, Bull. Chem. Soc. Jpn. 70 (1997) 1607.
[12] H.T. Evans, J.S. Showell, J. Am. Chem. Soc. 91 (1969) 3275.
[13] G.J. Siri, M.I. Morales, M.N. Blanco, H.J. Thomas, Appl. Catal. 19 (1985) 45.
[14] C.H. Giles, D. Smith, A.J. Huitson, J. Coll. Interface Sci. 47 (1974) 755.
[15] C.H. Giles, A.P. D'Silva, I.A. Easton, J. Coll. Interface Sci. 47 (1974) 766.
[16] J. Rodriguez-Carvajal, Pysica B 192 (1993) 55.
[17] A.B.P. Lever, Inorganic Electronic Spectroscopy, Elsevier, Amsterdam, 1984.
[18] R. Thomas, E.M. Van Oers, V.H.J. de Beer, J.A. Moulijn, J. Catal. 76 (1982) 241.
[19] C.I. Cabello, I.L. Botto, F. Cabrerizo, M.G. González, H.J. Thomas, Ads. Sci. Technol. 18 (7) (2000) 591.
[20] S. Kasztelan, E. Payen, H. Toulhoat, J. Grimblot, J.P. Bonnelle, Polyhedron 5 (1/2) (1986) 157.
[21] S. Kasztelan, H. Toulhoat, J. Grimblot, J.P. Bonnelle, Appl. Catal. 13 (1984) 127;
S. Kasztelan, H. Toulhoat, J. Grimblot, J.P. Bonnelle, Bull. Soc. Chim. Belg. 93 (1984) 807.
[22] H. Wise, Polyhedron 5 (1/2) (1986) 145.
[23] J.V. Lauritsen, S. Helveg, E. Laegsgaard, I. Stensgaard, B.S. Clausen, H. Topsøe, F. Besenbacher, J. Catal. 197 (2001) 1.
[24] M. Ternan, J. Catal. 104 (1987) 256.
[25] D. Pirotte, J.M. Zabala, P. Grange, B. Delmon, Bull. Soc. Chim. Belg. 90 (1981) 1239.